Understanding the relationship between crystal structure, plasticity and compaction behavior of theophylline, methyl gallate and their 1:1 cocrystal

Sayantan Chattoraj, Limin Shi and Changquan Calvin Sun

Supplementary Information

1. Phase purity of powders

Phase purity of the three powders was examined by comparing powder X-ray diffraction data (PXRD, Bruker AXS D5005, Madison, WI) with diffraction patterns calculated from corresponding single crystal structures, using Materials Studio 5.0 (Accelrys, San Diego, CA). For PXRD studies, a Cu X-ray source (45 kV, 40 mA) providing CuKα_1 emission of 1.5414 Å was used. Data were collected at 5 - 40^o 2θ at a step size of 0.01^o with a dwell time of 1s at each step. The reasonably good match between the experimental and calculated PXRD patterns, for all three powders, rule out gross phase contamination in these powders (Figure S1).

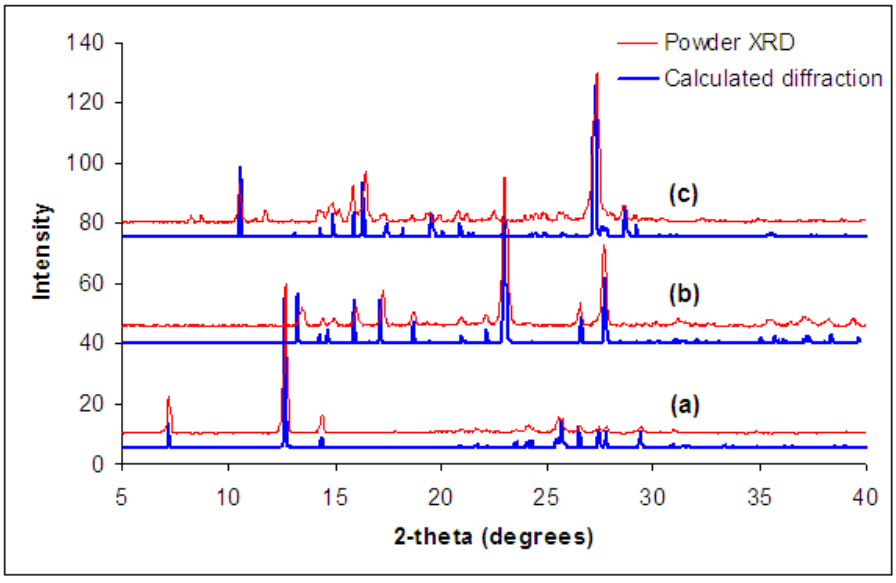

Figure S1. Calculated and experimental PXRD patterns of **(a)** theophylline, **(b)** methyl gallate, and **(c)** cocrystal

2. Compactibility of powders

Compactibility data show how tablet tensile strength depends on tablet porosity. Compactibility of each powder (Figure S2) was fitted using Ryshkewitch – Duckworth equation (equation 1):[1]

$$\sigma = \sigma_0 e^{-b\varepsilon} \qquad (1)$$

where σ is the tablet tensile strength at a particular porosity value, σ_0 is the tablet tensile strength extrapolated to zero porosity, b is a pre-exponential constant and ε is tablet porosity. Tablet porosity was calculated using out-of-die tablet densities (ρ_{tab}) and true densities (ρ_{true}) of the three materials, using equation 2: [2]

$$\varepsilon = 1 - \frac{\rho_{tab}}{\rho_{true}} \qquad (2)$$

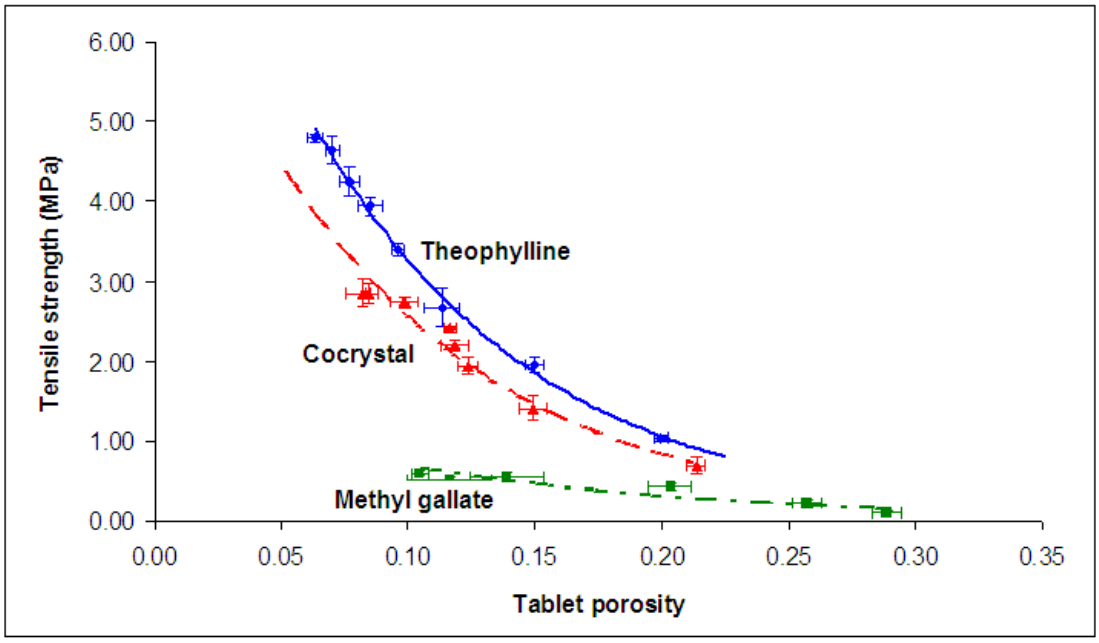

Figure S2. Compactibility of theophylline, methyl gallate, and cocrystal

As can be seen from Figure S2, similar to tabletability (Figure 2, main paper), theophylline's compactibility was significantly higher than cocrystal, while due to the poor compactibility of methyl gallate, tablets for methyl gallate could not be compacted below 0.10 tablet porosity. Using the Ryshkewitch-Duckworth equation[1], extrapolated tensile strength of theophylline at zero tablet porosity (σ_0) was calculated as 9.98 ± 0.36 MPa, while for the cocrystal, σ_0 was 8.81 ± 0.24 MPa. For methyl gallate, no attempt was made to extrapolate the compactibility plot to zero porosity.

3. Particle size and morphology effects on the compactibility of theophylline

To examine the effect of particle size and morphology on the compaction behavior of theophylline, we compared compactibility of three batches of theophylline. Batch 1 was commercial theophylline anhydrate powder with prism-shaped crystals (Figure S3, Batch 1). Batch 2 was prepared from commercial theophylline by cryomilling the powder under liquid nitrogen at 77K (SPEX SamplePrep 6750 Freezer/Mill, Metuchen, NJ; cryomilling conditions: pre-cooling (T_1) – 2 min, grinding (T_2) – 1 min, cooling (T_3) – 1 min, number of cycles – 2). We verified that the samples, immediately after cryomilling, did not show reduction in crystallinity, based on differential scanning calorimetry (model 2920, TA Instruments, New Castle, DE) and powder X-ray diffractometry (Bruker AXS D5005, Madison, WI) data. This behavior of cryomilled theophylline crystals, of undergoing minimal or no disorder during milling, is consistent with the literature.[3] For Batch 2, the powdered material was not subjected to any further treatment, and the compactibility was measured directly. The prism-shaped crystals of commercial theophylline were converted to crystals, having more iso-dimensional

morphology, in Batch 2 (Figure S3). For Batch 3, after following a similar cryomilling protocol as in Batch 2, the sample was suspended in ethanol with continuous stirring, using magnetic stirrer in a sealed round bottom flask. This treatment produced crystals of prism morphology, similar to commercial theophylline, but with significantly reduced average particle size.

Such drastic changes in particle size or morphology, however, did not significantly affect the compactibility of theophylline (Figure S4). Reduction in particle size slightly enhanced the compactibility of theophylline, as expected due to larger available bonding area[4]. However, compactibility was not affected by changes in crystal morphology.

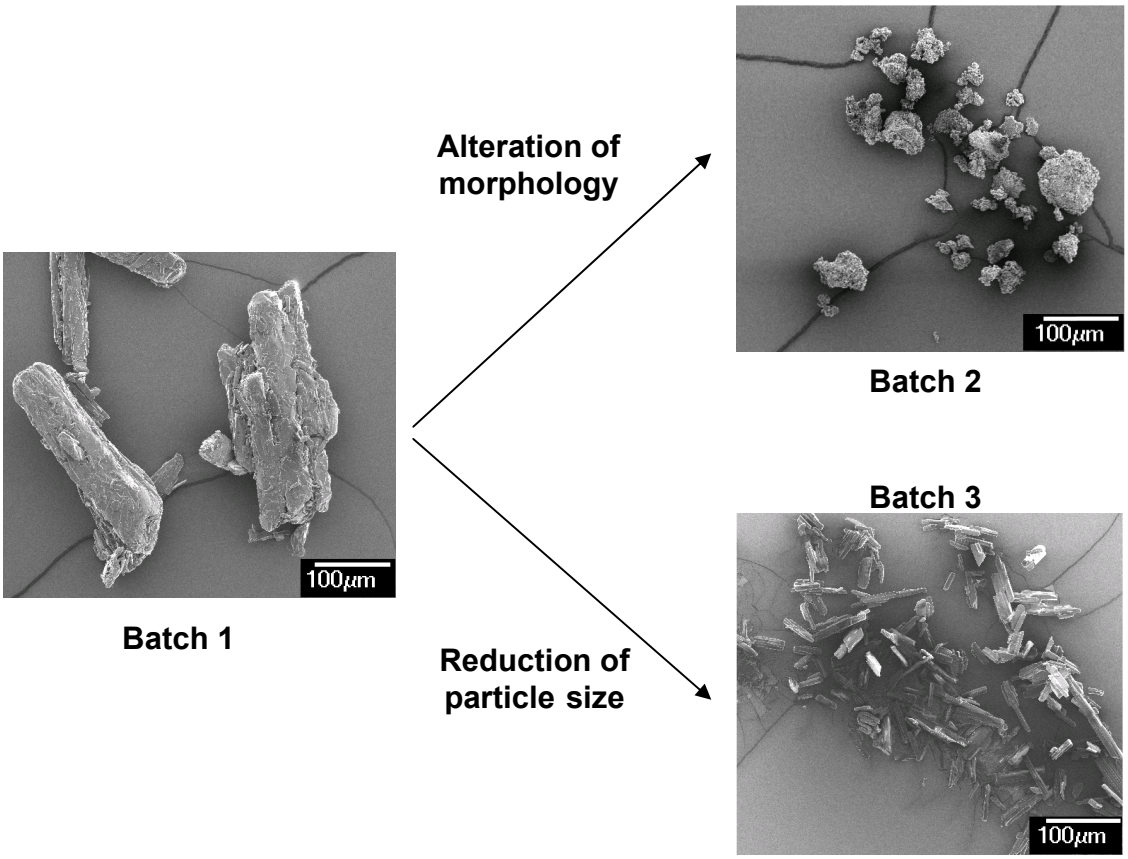

Figure S3. SEM images of the three batches of theophylline

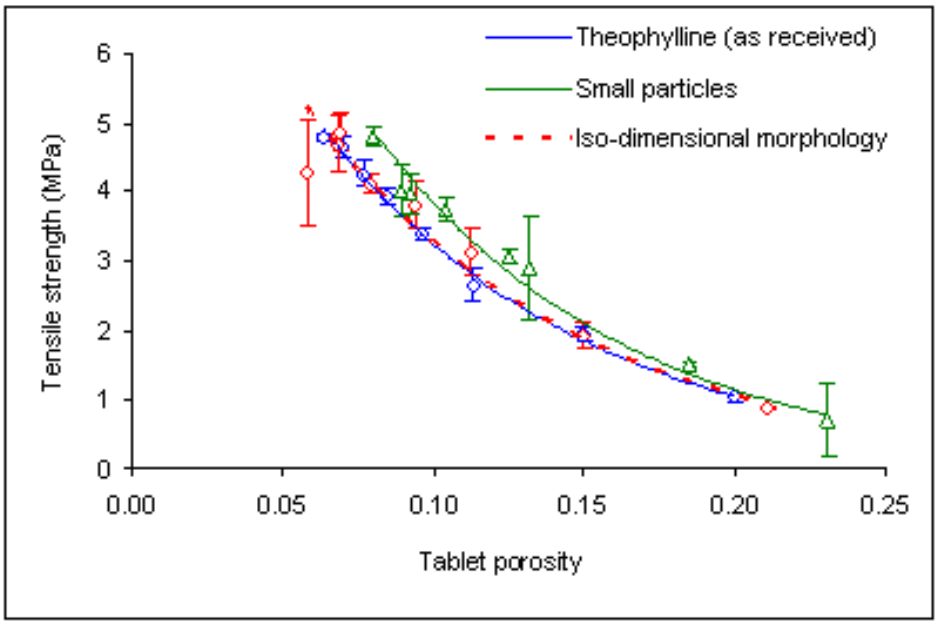

Figure S4. Compactibility of the three batches of theophylline

4. Crystal structure solution of methyl gallate

4.1. Data collection

A crystal (approximate dimensions 0.28 × 0.23 × 0.12 mm^3) was placed onto the tip of a 0.1 mm diameter glass capillary and mounted on a CCD area detector diffractometer for a data collection at 173(2) K.[5] The crystal structure of methyl gallate at 100 K has already been published,[6] and we here report a new determination at 173K. A preliminary set of cell constants was calculated from reflections harvested from three sets of 20 frames. These initial sets of frames were oriented such that orthogonal wedges of reciprocal space were surveyed. This produced initial orientation matrices determined from 46 reflections. The data collection was carried out using MoKα radiation (graphite

monochromator) with a frame time of 20 seconds and a detector distance of 4.9 cm. A randomly oriented region of reciprocal space was surveyed to the extent of one sphere and to a resolution of 0.84 Å. Four major sections of frames were collected with 0.30º steps in ω at four different ϕ settings and a detector position of -28º in 2θ. The intensity data were corrected for absorption and decay (SADABS).[7] Final cell constants were calculated from of 2951 strong reflections from the actual data collection after integration (SAINT).[8] In Table S1, additional crystal and refinement information are provided.

4.2. Structure solution and refinement

The structure was solved and refined using Bruker SHELXTL.[9] The space group $P2_1/n$ was determined based on systematic absences and intensity statistics. A direct-methods solution was calculated which provided most non-hydrogen atoms from the E-map. Full-matrix least squares / difference Fourier cycles were performed which located the remaining non-hydrogen atoms. All non-hydrogen atoms were refined with anisotropic displacement parameters. All hydrogen atoms were placed in ideal positions and refined as riding atoms with relative isotropic displacement parameters. In Table S2, information about hydrogen bonding in methyl gallate crystal is provided. The final full matrix least squares refinement converged to$R1 = 0.0469$ and$wR2 = 0.1380$ (F^2, all data). Thermal ellipsoid diagram of methyl gallate molecule at 50% probability is shown in Figure S5.

Empirical formula	$C_8 H_8 O_5$
Formula weight	184.14
Temperature	173(2) K
Wavelength	0.71073 Å
Crystal system	Monoclinic
Space group	$P2_1/n$
Unit cell dimensions	a = 7.6798(12) Å α = 90° b = 9.9854(15) Å β = 96.005(2)° c = 10.5949(16) Å γ = 90°
Volume	808.0(2) $Å^3$
Z	4
Density (calculated)	1.514 Mg/m^3
Absorption coefficient	0.128 mm^{-1}
***F*(000)**	384
Theta range for data collection	2.81 to 27.49°
Index ranges	$-9 \le h \le 9, 0 \le k \le 12, 0 \le l \le 13$
Reflections collected	7106
Independent reflections	1840 [R(int) = 0.0284]
Observed reflections	1404
Completeness to theta = 27.49°	99.5%
Absorption correction	Multi-scan
Max. and min. transmission	0.985 and 0.966
Refinement method	Full-matrix least-squares on F^2
Data / restraints / parameters	1840 / 0 / 122
Goodness-of-fit on F^2	1.085
Final *R* indices [*I*>2sigma(*I*)]	$R1$ = 0.0469, $wR2$ = 0.1255
***R* indices (all data)**	$R1$ = 0.0621, $wR2$ = 0.1380
Largest diff. peak and hole	0.243 and -0.310 e.$Å^{-3}$

Table S1. Crystal data and structure refinement for methyl gallate

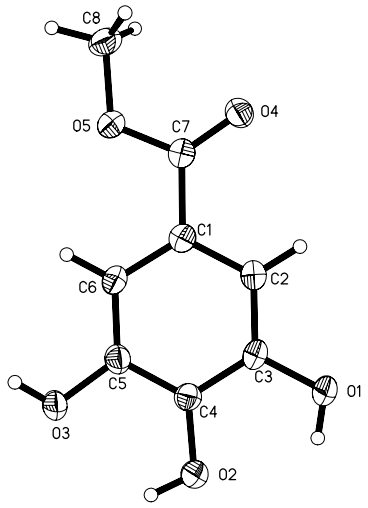

Figure S5. Thermal ellipsoid of methyl gallate at 50% probability with the atoms labeled (C-carbon, O-oxygen)

H-bond between atoms D-H...A	Distance between atoms			Angle
	d(D-H) [Å]	d(H...A) [Å]	D(D...A) [Å]	<(DHA) [°]
O1-H1A...O4#1	0.84	2.00	2.7113(16)	142.5
O2-H2A...O4#2	0.84	2.16	2.9587(16)	159.7
O3-H3A...O1#3	0.84	1.87	2.6894(16)	166.5

Symmetry transformations used to generate equivalent atoms:
#1 -x+1/2,y-1/2,-z+3/2 #2 x-1/2,-y+1/2,z-1/2
#3 x+1/2,-y+1/2,z-1/2

Table S2. Hydrogen bonds in methyl gallate

5. Crystal structure solution of theophylline-methyl gallate (1:1) cocrystal

5.1. Data collection

A crystal (approximate dimensions 0.45 x 0.18 x 0.18 mm^3) was placed onto the tip of a

0.1 mm diameter glass capillary and mounted on a Siemens SMART platform CCD diffractometer for a data collection at 173 K.[5] A preliminary set of cell constants was calculated from reflections harvested from three sets of 20 frames. These initial sets of frames were oriented such that orthogonal wedges of reciprocal space were surveyed. This produced initial orientation matrices. The data collection was carried out using MoKα radiation (graphite monochromator) with a frame time of 30 seconds and a detector distance of 4.18 cm. A randomly oriented region of reciprocal space was surveyed to the extent of one sphere and to a resolution of 0.84 Å. Four major sections of frames were collected with 0.30º steps in ω at four different ϕ settings and a detector position of -28º in 2θ. The intensity data were corrected for absorption and decay (SADABS).[7] Final cell constants were calculated from the actual data collection after integration (SAINT).[8] Refer to Table S3 for additional crystal and refinement information.

5.2. Structure solution and refinement

The structure was solved and refined using SHELXS-97 [9] with Sir97.[10] The space group $P2_1/c$ was determined based on systematic absences and intensity statistics. Structure solution using direct methods in SHELXTL initially did not result in acceptable crystal structure, which may be attributed to the stacking flat sheet-like structures that the molecules form. Sir97 from WinGx was used to generate an automatic structure solution with the given data. Atom position assignment was verified in SHELXTL. Full-matrix least squares / difference Fourier cycles were performed. All non-hydrogen atoms were refined with anisotropic displacement parameters. All hydrogen atoms were placed in

ideal positions and refined as riding atoms with relative isotropic displacement parameters. As hydrogen bonds played crucial role in this crystal structure, a hydrogen bond table was generated using EQIV and HTAB commands. No disorder modeling was necessary. The final full matrix least squares refinement without disorder modeling converged to $R1 = 0.0604$ and $wR2 = 0.1855$ (F^2, all data). The goodness-of-fit was 1.000.

The cocrystal belongs to space group $P2_1/c$. Hydrogen bonding between constituent atoms played a major role in the formation of the structure. Presence of a number of hydrogen bond donors and acceptors like the nitrogen and oxygen atoms in the molecules make this crystal structure very amenable to hydrogen bond formation. Table S4 shows the relevant data regarding hydrogen bonding in this structure.

Table S3. Crystal data and structure refinement for cocrystal.

Empirical formula	$C_7 H_8 N_4 O_2$, $C_8 H_8 O_5$	
Formula weight	364.32	
Temperature	173 K	
Wavelength	0.71073 Å	
Crystal system	Monoclinic	
Space group	$P2_1/c$	
Unit cell dimensions	a = 10.2745(7) Å	α = 90°
	b = 10.1246(7) Å	β = 98.865°
	c = 14.8789(10) Å	γ = 90°
Volume	1529.29 Å^3	
Z	4	
Density (calculated)	1.582 mg/m^3	
Absorption coefficient	0.128 mm^{-1}	
F(000)	760	
Crystal color, morphology	Colorless, Block	
Crystal size	0.45 x 0.18 x 0.18 mm^3	
Theta range for data collection	2.01 to 25.12°	
Index ranges	$-12 \le h \le 12$, $-12 \le k \le 12$, $-17 \le l \le 16$	
Reflections collected	11139	
Independent reflections	2724 [R(int) = 0.0428]	
Observed reflections	1720	
Completeness to theta = 25.12°	100.0%	
Absorption correction	Multi-scan	
Max. and min. transmission	0.9774 and 0.9448	
Refinement method	Full-matrix least-squares on F^2	
Data / restraints / parameters	2724 / 0 / 242	

Goodness-of-fit on F^2	1.000
Final R indices [I>2sigma(I)]	$R1$ = 0.0604, $wR2$ = 0.1579
R indices (all data)	$R1$ = 0.0954, $wR2$ = 0.1855
Largest diff. peak and hole	0.504 and -0.390 e.Å^{-3}

Table S4. Hydrogen bonds for cocrystal [Å and °].

D-H...A	d(D-H)	d(H...A)	d(D...A)	<(DHA)
O3-H3A...O1#1	0.84	1.91	2.750(3)	177.1
O4-H4A...N3	0.84	2.03	2.803(3)	151.8
O4-H4A...O3	0.84	2.29	2.723(2)	112.8
O5-H5B...O6#2	0.84	1.90	2.726(3)	166.4
N4-H4B...O2#3	0.88	1.85	2.713(3)	168.1

Symmetry transformations used to generate equivalent atoms:

#1 x,y-1,z #2 -x+1,y+1/2,-z+1/2 #3 -x+2,-y+1,-z+2

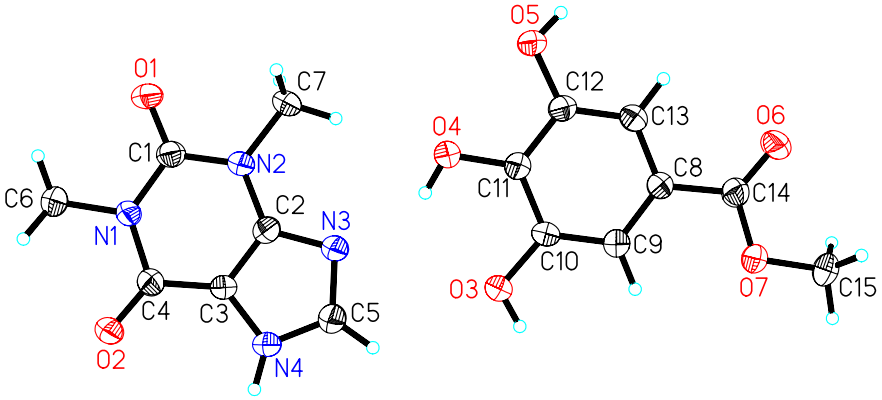

Figure S6: Thermal ellipsoid of cocrystal at 50% probability (C-carbon, O-oxygen, N-nitrogen)

Acknowledgements

We are grateful to Dr. Victor G. Young Jr. for solving the single crystal structure of methyl gallate. The work was conducted at the X-Ray Crystallographic Laboratory, S146 Kolthoff Hall, Department of Chemistry, University of Minnesota. We also thank the I.T. Characterization Facility of University of Minnesota for instrument support to our powder X-ray diffractometry studies.

References

1 E. Ryshkewitch, *J Amer Ceramic Soc*, 1953, 36, 65-68.
2 C. K. Tye, C. C. Sun & G. E. Amidon, *J. Pharm. Sci.*, 2005, 94, 465 - 472.
3 Y. Lin, R. P. Coggill & P. L. D. Wildfong, *J. Pharm. Sci.*, 2009, 98, 2696 - 2708.
4 C. C. Sun, *J. Pharm. Sci.*, 2009, 98, 1671 - 1687.
5 SMART. V5.054 Bruker Analytical X-raySystems, Madison, WI, 2001.
6 D. Bebout and S. Pagola, *Acta Cryst E*, 2009, E65, 317-318.
7 R. Blessing, *Acta Cryst. A*, 1995, 51, 33-38.
8 SAINT+. V6.45, Bruker Analytical X-Ray Systems, Madison, WI, 2003.
9 SHELXTL. V6.14, Bruker Analytical X-Ray Systems, Madison, WI 2000.
10 A. Altomare, M. C. Burla, M. Camalli, G. Cascarano, C. Giacovazzo, A. Guagliardi, A. G. G. Moliterni, G. Polidori & R. Spagna. *J. Appl. Cryst.* 1998, 32**,** 115.